NANO · MICRO small
www.small-journal.com

Zebrafish Embryos Allow Prediction of Nanoparticle Circulation Times in Mice and Facilitate Quantification of Nanoparticle–Cell Interactions

*Nils-Jørgen Knudsen Dal, Agnese Kocere, Jens Wohlmann, Simon Van Herck, Tobias A. Bauer, Julien Resseguier, Shahla Bagherifam, Hilde Hyldmo, Matthias Barz, Bruno G. De Geest, and Federico Fenaroli**

The zebrafish embryo is a vertebrate well suited for visualizing nanoparticles at high resolution in live animals. Its optical transparency and genetic versatility allow noninvasive, real-time observations of vascular flow of nanoparticles and their interactions with cells throughout the body. As a consequence, this system enables the acquisition of quantitative data that are difficult to obtain in rodents. Until now, a few studies using the zebrafish model have only described semiquantitative results on key nanoparticle parameters. Here, a MACRO dedicated to automated quantitative methods is described for analyzing important parameters of nanoparticle behavior, such as circulation time and interactions with key target cells, macrophages, and endothelial cells. Direct comparison of four nanoparticle (NP) formulations in zebrafish embryos and mice reveals that data obtained in zebrafish can be used to predict NPs' behavior in the mouse model. NPs having long or short blood circulation in rodents behave similarly in the zebrafish embryo, with low circulation times being a consequence of NP uptake into macrophages or endothelial cells. It is proposed that the zebrafish embryo has the potential to become an important intermediate screening system for nanoparticle research to bridge the gap between cell culture studies and preclinical rodent models such as the mouse.

1. Introduction

The zebrafish embryo is rapidly becoming an attractive tool for screening nanoparticles.[1] This transparent vertebrate system develops rapidly, and already after 48 h a beating heart and robust blood circulation are readily observable under a stereomicroscope.[2] Intravenously injected fluorescent nanoparticles (NPs) can therefore be directly observed at the whole animal level.[3] In addition, the availability of several fluorescent transgenic zebrafish lines with selectively labeled cells allows the assessment of NP interactions with important cells such as macrophages and endothelial cells.[3–5] These characteristics, together with the much lower costs of maintenance in comparison to murine models, place the zebrafish in an ideal position to become an important intermediate system for screening NPs between cell cultures and mice. However, only semiquantitative methods for NP analysis have been applied until now, using confocal microscopy, which is more time consuming than the use of a stereomicroscope and therefore allows fewer animals to be analyzed.[6,7] Among the parameters that are crucial for understanding NP behavior is the circulation time. This factor, which can also be studied in adult zebrafish, is essential for designing new nanomaterials since a long circulation time is associated with increased accumulation at diseased sites in

N.-J. K. Dal, A. Kocere, J. Wohlmann, Dr. J. Resseguier, H. Hyldmo, Dr. F. Fenaroli
Department of Biosciences
University of Oslo
Blindernveien 31, 0371 Oslo, Norway
E-mail: federico.fenaroli@ibv.uio.no
Dr. S. Van Herck, Prof. B. G. De Geest
Department of Pharmaceutics
Ghent University
Ottergemsesteenweg 460, 9000 Ghent, Belgium
The ORCID identification number(s) for the author(s) of this article can be found under https://doi.org/10.1002/smll.201906719.

DOI: 10.1002/smll.201906719

T. A. Bauer, Dr. M. Barz
Institute for Organic Chemistry
Johannes Gutenberg-University Mainz
Duesbergweg 10–14, 55099 Mainz, Germany
Dr. S. Bagherifam
Department of Radiation Biology
Institute for Cancer Research
Norwegian Radium Hospital
Montebello, N-0310 Oslo, Norway

cancer and tuberculosis.[8–10] NP flow is greatly influenced by their uptake into blood macrophages (or monocytes). Moreover, for nanocarriers destined for the cancer therapy, uptake by macrophages is generally considered to decrease the chances of accumulation in tumor sites and is therefore considered a detrimental factor for therapeutic efficiency. However, some recent reviews and publications[11,12] suggest that direct targeting of some macrophages may be desirable since a subset of these cells can be selectively recruited to diseased sites, such as tumor-associated macrophages (TAMs) in solid tumors.[13–15] Moreover, a number of intracellular pathogens reside and replicate within macrophages, and several publications now recognize the importance of targeting this cell type using NPs for fighting intracellular infections.[16,17] This approach has been reported for *Mycobacterium marinum*,[4] *Francisella novicida*,[18] *Staphylococcus aureus*,[19] and *Salmonella enterica*.[20]

Another important cell type that affects NP distribution is endothelial cells, which line the blood vessels through which NP flow along the body; by binding and taking up NPs, they are also capable of influencing their circulation times. This phenomenon is not easily noticed in mouse models. Even in the zebrafish, only a few studies have described the uptake of NPs into endothelial cells in vivo.[3,21] Although uptake into endothelial cells may be undesirable since they reduce circulation time, some researchers have added specific ligands to NPs in order to enhance this process, targeting specific diseases such as thrombosis and ischemia.[22,23]

Here, we describe methods to reliably quantify NP (see **Table 1**) circulation time and estimate the relative accumulation of NPs in macrophages or endothelial cells in the zebrafish embryo using a stereomicroscope and a user-friendly imageJ MACRO for automated image analysis. From the seven NP formulations, four were selected to compare NP circulation time in zebrafish with mice.

2. Experimental Section

2.1. Zebrafish Embryo Handling

In this study, different strains of zebrafish embryos were used. For the manual analysis of the circulation (MACRO manual circulation), wild-type (WT) zebrafish embryos were used. For the automatic analysis of the circulation (MACRO automatic analysis) zebrafish expressing enhanced green fluorescence protein (EGFP) in the vasculature, Tg(fli1a:EGFP), were used; for the macrophage uptake analysis (MACRO macrophage uptake): Tg(mpeg1:cherry); and for the endothelial uptake analysis (MACRO endothelial uptake): double transgenic Tg(mpeg1:cherry) and Tg(fli1a:EGFP). After fertilization, the harvested embryos were kept at 28.5 °C in zebrafish egg water containing phenylthiourea (0.003%). All experiments were approved by the Norwegian authorities regulating animal research.

2.2. Nanoparticle Preparations

2.2.1. Liposomes

Phosphatidyl choline (PC) was bought from Lipoid (product E PC-3), cholesterol (Chol) from Sigma, while phosphoethanolamine polyethylene glycol (PEG) 2000 (PE-PEG) and ATTO633-1,2-dioleoyl-sn-glycero-3-phosphoethanolamine (DOPE) from ATTO-TEC, and biotinyl phosphoethanolamine (B-PE) from Avanti Lipids (products 880120P and 870282).

Procedure: 3 mL of chloroform and 5 µL of a solution 1 mg mL^{-1} in ethanol of ATTO-633-labeled DOPE were added to a flask containing 2.4 mg of PC, 0.64 mg of Chol, and 0.69 mg of PE-PEG for PEGylated liposomes without biotin; 2.3 mg of PC, 0.1 mg of B-PE, 0.64 mg of Chol, and 0.69 mg of PE-PEG for PEGylated liposomes with biotin; or 3.09 mg of PC and 0.64 mg of Chol for non-PEGylated liposomes.

These mixtures were dried using a rotatory evaporator in three consecutive steps: 150 mbar for 30 min, 80 mbar for 30 min, and 16 mbar for 10 min. The dried phospholipids were then hydrated with 1 mL of phosphate-buffered saline (PBS) at 70 °C and vortexed thoroughly. The resuspended mixture was then introduced in a gas-tight syringe which allowed the passage of the solution through filters of different sizes mounted on a mini extruder (Avanti lipids) at 70 °C. For liposomes 100 nm PEG and 99 nm PEG biotin, a 0.05 µm pore size was used, while for liposomes 580 nm PEG and 623 nm NO PEG, a 0.8 µm filter was used. Liposomes were analyzed by dynamic light scattering (DLS) and a Zetasizer.

2.2.2. Poly(Sar-b-pCys(SO_2Et)) NP

The preparation of core cross-linked polymeric micelles was adapted from the literature and modified.[24] Poly(sarcosine)-*b*-poly((*S*-ethylsulfonyl)cysteine) ($pSar_{225}$-*b*-$pCys(SO_2Et)_{31}$) was

Table 1. NPs used in the study. Hydrodynamic diameter measures the peak intensity obtained by DLS.

NP type	Hydrodynamic diameter (D_h) [nm]	Polydispersity index (PDI)	Zeta potential [mV]
1) PEGylated liposomes	100 ± 0.55	0.04 ± 0.01	−3.54 ± 1.19
2) PEGylated liposomes with biotin	99 ± 0.58	0.07 ± 0.02	−1.49 ± 0.59
3) PEGylated liposomes	580.9 ± 12	0.4 ± 0.07	−1.53 ± 0.96
4) Non-PEGylated liposomes	623.7 ± 12	0.37 ± 0.06	−5.12 ± 0.81
5) Poly(DMA-*b*-BzKetAc) NP	65.8 ± 0.6	0.174 ± 0.0006	−28.9 ± 16
6) Poly(Sar-*b*-pCys(SO_2Et)) NP	86.1 ± 0.93	0.131 ± 0.007	−1.94 ± 3.84
7) Poly(Sar-*b*-pCys(SO_2Et)) NP	47.4 ± 0.45	0.094 ± 0.001	−3.36 ± 5.86

dissolved in dimethyl sulfoxide (DMSO) at a concentration of 7.5 g L^{-1} for 1 h. Next, 20 vol% of 1×10^{-3} M acetate buffer (pH 4.75) was added to adjust the concentration to 6.6 g L^{-1}. The solution was left to equilibrate at room temperature for 5 h, followed by dialysis against 1×10^{-3} M acetate buffer (pH 4.75). The solution was filtered (GHP 450) and concentrated to 6.6 g L^{-1} by spin filtration (Amicon Ultra, molecular weight cut-off (MWCO) = 3 kDa), yielding the micelle solution. For the preparation of nanoparticle type 7 (Table 1), DMSO and acetate buffer were equipped with 1 and 10×10^{-3} M thiourea, respectively. For cross-linking, in a separate flask, the liponamide cross-linker was dissolved in ethanol at a concentration of $\beta = 10$ g L^{-1} and one equivalent of an aqueous solution of tris(2-carboxyethyl)phosphine hydrochloride (TCEP·HCl) (50 g L^{-1}) was added per disulfide. After 18 h, the cross-linker solution was added to the micelle solution at equimolar amounts of thiols per cysteines. The reaction mixture was allowed to stand at room temperature for 48 h. To remove residual cross-linker and free polymer, the solution was dialyzed against DMSO and MilliQ water (MWCO = 6–8 kDa), followed by repetitive spin filtration (Amicon Ultra, MWCO = 100 kDa). For labeling, 1.0 equivalent of cyanine 5 NHS–ester stock solution (0.3 eq of Atto647N NHS-ester for NP7) in DMSO (5 g L^{-1}) was added per polymer end group at pH 7.4 (adjusted with 1 M $NaHCO_3$ solution). After 72 h, excess dye was removed by repetitive spin filtration (Amicon Ultra, 100 kDa) using ethanol/water mixtures, and the final particle solution (in MilliQ water) was stored at 4 °C. The absence of free polymer and free dye was verified by gel permeation chromatography in hexafluoro isopropanol.

The preparation of poly(*N*,*N*-dimethylacrylamide)-*b*-poly(2-((2-(benzyloxy)propan-2-yl)oxy)ethyl acrylate) (poly(DMA-*b*-BzKetAc))) NP was performed according the method described in ref. [10].

2.3. Nanoparticle Injections

In order to intravenously inject the zebrafish embryos, NP solutions (4 mg mL^{-1}) were loaded into borosilicate needles (GC100T-10, Harvard instruments) previously prepared using a micropipette puller (P-97, Sutter instruments). The needles were then attached to an Eppendorf Femtojet Express microinjector and controlled by a Narishige MN-153 micromanipulator. The injection of a precise quantity of NPs was done by careful manipulation of the pressure and time of injection. Once the desired volume was achieved, zebrafish embryos were anesthetized using zebrafish egg water supplemented with tricaine (0.02%). The injection of these embryo occurred on a Petri dish that had previously been filled with a solution of 2% agarose, which solidifies upon cooling. All the injections were made in the posterior cardinal vein at 2 days post fertilization.

2.4. Imaging of Zebrafish Embryos

Each zebrafish embryo injected with NPs was subsequently imaged at different times and in different channels depending on the type of analysis, using a Leica stereomicroscope DFC365FX (1.0× planapo lens) obtaining images of both the caudal region (120× magnification) and the whole fish (30× magnification). Prior to the imaging session, zebrafish were kept in Petri dishes wrapped in aluminum foil to avoid any possible photobleaching.

- *For Circulation Time, Manual*: Images were taken at 5 min and at 1, 4, 8, 24, 48, and 72 h, in transmission and the far red (Cy5, NP) fluorescence channel.
- *For Circulation Time, Automatic*: Images were taken at 5 min and at 1, 4, 8, 24, 48, and 72 h, in transmission, far red (Cy5, NP), and green (green fluorescence protein (GFP), endothelium) fluorescence channels.
- *For Macrophage Uptake Evaluation, Automatic*: Images were taken at 6 h in transmission, far red (Cy5, NP), and red (DsRed, macrophage) fluorescence channels.
- *For Endothelial Uptake Evaluation, Automatic*: Images were taken at 6 h in transmission, far red (Cy5, NP), red (DsRed, macrophage), and green (GFP, endothelium) fluorescence channels.

2.5. Functioning of the ImageJ MACRO

The ImageJ MACRO is available at https://github.com/wohlmann/IJ_ZF_NP_Quantification.

Once started, the MACRO will ask, via a file handling dialogue, the folder where the images to be analyzed are stored and another folder, where the output results will become available. The Leica *.lif format or *.tif images will be accepted by the MACRO file handling.

As the MACRO includes various types of analyses, a second dialogue will enable the selection of the desired analysis as well as the definition of an individual channel order and assignment. Analysis options are 1) circulation times, manual; 2) circulation times, automatic; 3) macrophage uptake, automatic; or 4) endothelial uptake, automatic. Fluorescent channels will be assigned to 1) transmission image, 2) NP, 3) macrophage, or 4) endothelium fluorescence.

Additionally, the user has the option to verify the measurements by analyzing quality control output images for the detected regions of interest (ROIs). If the images are not satisfactory, the levels of thresholding of each analysis can also be customized.

2.5.1. Circulation Time Analysis: Manual

After automatic sorting of the images depending on the magnification, the MACRO will open and show the higher magnification images (120× magnification images) as well as predefined rectangles of adaptable number and size to be positioned on the caudal vein by the user as indicated in **Figure 1**C. After positioning the rectangles on the caudal artery, the MACRO will measure the fluorescence intensity in this region and compare it to the fluorescence intensity of the whole fish (30× magnification images) detected via its transmission signal. The results will be stored in two individual *.txt files (usable by spreadsheet software) for each measurement. The use of these values to determine NP circulation is explained in section "Quantification of the Results Obtained Using the MACRO."

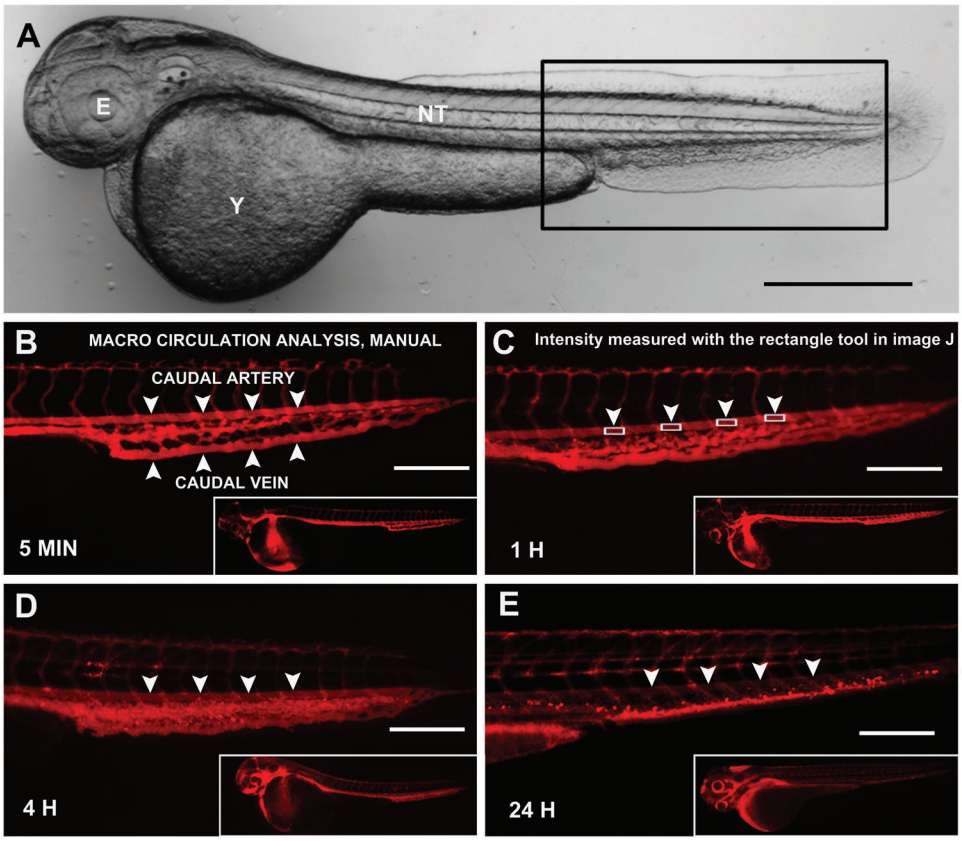

Figure 1. Circulation of NPs in the zebrafish embryo, manual analysis. A) Acquisition of the zebrafish embryo at 48 h post fertilization in the transmission channel; the rectangular inset shows the area where the caudal region images were taken. B–E) Images of the caudal vein of zebrafish injected with fluorescent NPs (here 100 nm liposomes with PEG) imaged at different time points—B) 5 min, C)1 h, D) 4 h, and E) 24 h. B) The main blood components of the caudal region are shown by arrowheads (caudal artery and caudal vein). C) The rectangles used for quantification of fluorescence are shown (arrowheads); these are either manually or automatically placed on the caudal artery and in between intersegmental vessels. D,E) The decrease in fluorescence of the caudal artery (arrowheads) can be seen at 4 and 24 h. B–E, insets) The values for fluorescence in the artery are normalized relative to the overall NP fluorescence in the whole fish. Scale bars: A) 500 nm and B–E) 200 nm.

2.5.2. Circulation Time Analysis: Automatic

In this type of analysis, the MACRO is utilizing the vasculature fluorescence (Tgfli1a:EGFP) signal to automatically detect the caudal vein region(120× magnification images). This detection was based on the muscle segments between the intersegmental vessels (ISVs) branching from the caudal vein and artery relying on an initial automated orientation of the image using the characteristic anatomical features of the zebrafish tail region. The rectangles for the measurement were adjusted to avoid inclusion of branching ISVs or local accumulations using a NP signal threshold and particle analysis. As for the manual analysis, the fluorescence intensity of the whole animal was also analyzed (30× magnification images). The results were stored in two individual *.txt files (usable by spreadsheet software) for each measurement. The use of these values to determine NP circulation is explained in section "Quantification of the Results Obtained Using the MACRO."

2.5.3. Macrophage Uptake Analysis: Automatic

In this analysis, the MACRO will first provide a thresholding of the NP signal (in 120× magnification images) in order to separate free NPs in the blood flow from the ones that have been taken up by cells; the latter, depending on the amount taken up, appear as brighter spots with higher density. Second, the macrophage signal was thresholded and overlapped with the NPs, and only the NPs within macrophages were analyzed for their intensity value. Similar to the NP circulation analysis, the overall NP fluorescence in the zebrafish was measured (30× magnification images) and the results were stored in two individual *.txt files (usable by spreadsheet software).

2.5.4. Endothelial Cells Uptake Analysis: Automatic

Identical to the macrophage uptake analysis, NPs and macrophages were thresholded but in this case, the NPs within macrophages were eliminated before the fluorescence intensity of the thresholded area occupied by the endothelium was measured for the remaining NP signals (120× magnification images). After the analysis of the whole zebrafish fluorescence (30× magnification images) in the NP channel, the results were stored in two individual *.txt files (usable by spreadsheet software) and will contain the estimated uptake of NPs by the endothelium in the caudal area and the overall fluorescence values in the whole zebrafish.

2.6. Further Details About the MACRO

Throughout the MACRO script, several comment lines were used to explain in detail every command.

2.7. Quantification of the Results Obtained Using the MACRO

The output *.txt files obtained from the MACRO contained, for each zebrafish embryo, two values that will be used for the subsequent analyses: the "mean fluorescence value," used for circulation analysis, and the "Raw Integrated Density" (RawIntDen), which is instead used for either macrophage or endothelial uptake and represents the sum of the pixel values in the selected area.

2.7.1. Circulation Analysis: Automatic and Manual

Raw Values: In this analysis for each time point the "mean fluorescence intensity" of the artery (M_{artery}, calculated from a 120× magnification image of the caudal region), and the "mean fluorescence values" of the whole zebrafish (M_{whole}, calculated from a 30× magnification image of the whole animal) were detected. Each point in the graph is represented by the result of the equation: $M_{\text{artery}}/M_{\text{whole}}$.

Percent Conversion: In order to convert results into percentages the value of each NP obtained at 5 min, M_{artery} (5 min)/M_{whole} (5 min) was considered the 100% estimate while the intensity of the background was considered to represent 0%. Thus, the percentage values are obtained as follows

$$\text{Flowing NP, percent} = \frac{\dfrac{M_{\text{artery}}\,(\text{time } x)}{M_{\text{whole}}\,(\text{time } x)} - \text{Background value}}{\dfrac{M_{\text{artery}}\,(5\text{ min})}{M_{\text{whole}}\,(5\text{ min})} - \text{Background value}} \times 100 \tag{1}$$

2.7.2. Scoring Macrophage and Endothelial Uptake of Nanoparticles

While for circulation analysis, the mean values of intensity were used, for both macrophage and endothelial analyses RawIntDen was utilized. The RawIntDen of each zebrafish caudal region (120× magnification images) was normalized by the overall fluorescence of the whole fish (also a RawIntDen value, 30× magnification images) and multiplied by 100.

Macrophage Uptake: The fluorescence of the pixels relative to NP fluorescence in the macrophage selection was expressed as the RawIntDen value obtained in the results file for each zebrafish embryo ($\text{RID}_{\text{macrophages}}$). The overall fluorescence intensity of NPs in the whole fish was also calculated as RawIntDen value ($\text{RID}_{\text{whole}}$). In order to obtain the final value, RIDmacrophages was normalized by RIDwhole and multiplied by 100 as shown below

$$\text{Macrophage uptake of NP} = \frac{\text{RID}_{\text{macrophages}}}{\text{RID}_{\text{whole}}} \times 100 \tag{2}$$

Endothelial Uptake: Just as for the macrophage analysis, the fluorescence of the pixels of the NPs which overlap with the endothelium signal was scored as a RawIntDen in the results file for each zebrafish ($\text{RID}_{\text{endothelium}}$). This value was normalized by the overall NP fluorescence ($\text{RID}_{\text{whole}}$) and multiplied by 100 as shown below

$$\text{Endothelial uptake of NP} = \frac{\text{RID}_{\text{endothelium}}}{\text{RID}_{\text{whole}}} \times 100 \tag{3}$$

2.8. Mouse Nanoparticle Circulation Analysis

Prior to the experiment, 6 week old male BALB/cAnNRj mice were divided into groups of six animals per cage according to the type of NPs (100 and 580 nm PEGylated liposomes, 623 nm non-PEGylated liposomes and 47 nm poly(Sar-*b*-pCys(SO_2Et) NP) and time point for blood sampling (5 min, 4 h, 24 h, and 72 h). Next, after 1 week of acclimatization, the mice received a single intravenous injection (200 µL) of NPs or with isotonic PBS solution (control). At the selected time points, the animals were placed under deep anesthesia (Isoflurane 5%) and after the ribcage was exposed, blood extraction was performed by cardiac puncture. This was followed by cervical dislocation to terminate the animals. Heparin-coated syringes and Eppendorf tubes were applied to prevent blood clotting. Samples were put on ice and protected from light by aluminum foil. 5 µL of blood from each animal was inserted into a fluorinated ethylene–propylene (FEP) tube, and an image in the far-red channel was taken with a Leica stereomicroscope DFC365FX. Mice receiving PBS were used as a background control. The NP circulation at each time point was then calculated as

$$\text{Flowing NP, percent} = \frac{\text{Fluorescence}\,(\text{time } x) - \text{Background value}}{\text{Fluorescence}\,(5\text{ min}) - \text{Background value}} \times 100 \tag{4}$$

Values obtained at 5 min and subtracted of the background were considered the 100% value while the background corresponded to the 0%. Mice experiments were approved by the Norwegian Food Safety Authority, Mattilsynet, FOTS ID: 20607.

2.9. Statistics Used

One-way analysis of variance (ANOVA) was used with Tukey's multicomparison test to compare the different groups for macrophage and endothelial uptake. The test was used to assess if the values come from a Gaussian distribution was the Kolmogorov–Smirnov test with Dallal–Wilkinson–Lille for *P*-value.

3. Results

3.1. Nanoparticle Circulation

The zebrafish embryo can be used to assess the circulation properties of NPs and here we have established two methods,

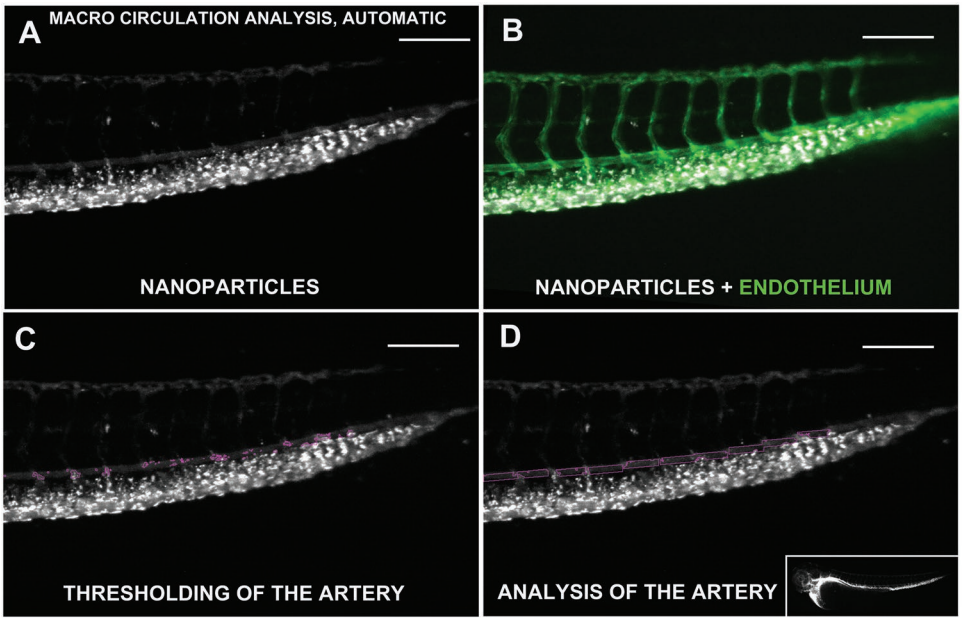

Figure 2. Circulation of NPs in the zebrafish embryo, automatic analysis. This image shows the steps performed by the MACRO for the analysis of the fluorescence in the caudal artery. A) The image processing of zebrafish injected with fluorescent NPs (99 nm PEGylated liposomes with biotin) utilizes B) the fluorescent signal of the vasculature to identify the caudal artery. C) Fluorescence due to NP uptake in the artery is removed, and D) regions in between intersegmental vessels are automatically detected to calculate the relative fluorescence. The results are then normalized relative to the fluorescence of the whole fish (panel (D), lower right image).

one manual and one automatic, to rapidly analyze the images. For this, we focused on the caudal region of the zebrafish which, being relatively thin, allows for better imaging and therefore more precise results compared to other sites in the zebrafish embryo. The main blood components of the caudal region are the caudal vein, the site of NP injection, and the caudal artery, the site of importance for the measurements (Figure 1B, arrowheads). In Figure 1, we show zebrafish embryos that had been injected with 100 nm PEG liposomes with images of the caudal area (Figure 1A) at different time points: 5 min (Figure 1B), 1 h (Figure 1C), 4 h (Figure 1D), and 24 h (Figure 1E). In order to evaluate the circulation time, we measured the average fluorescence of the caudal artery over time, as this relatively big vessel facilitates the analysis due to its size and the absence of NP uptake by macrophages and lower uptake by endothelial cells, which occurs mainly in the caudal vein. As illustrated in Figure 1, the fluorescence signal due to flowing 100 nm PEGylated liposomes in the caudal vein decreases in time. Using the manual option of the MACRO, the user will place rectangles of predefined number and size on the caudal artery, between the intersegmental vessels (as shown in Figure 1B) for the analysis of the fluorescence signal. The MACRO will then automatically measure the fluorescence intensity of the resulting region as well as the whole fish region detected via its transmission signal.

In the automatic circulation analysis (**Figure 2**), it is necessary to use transgenic zebrafish possessing fluorescent vasculature, here we used the Tg(fli1a:EGFP) strain. The information obtained from the blood endothelium is used by the MACRO to detect the regions of the artery contained between two intersegmental vessels (Figure 2B). These regions will be analyzed while areas characterized by high fluorescence, due to endothelial uptake, will be eliminated from the quantification, as shown in Figure 2C. As for the previous analysis, the mean fluorescence intensity in these areas will be measured (Figure 2D) together with the total fluorescence of the whole embryo; the relative values of each zebrafish are provided in two separate *.txt files.

In order to plot the circulation in time (5 min, 1 h, 4 h, 8 h, 24 h, 48 h, and 72 h), the average fluorescence signal in the artery is normalized relative to the overall fluorescence (see "Experimental Section" for details), resulting in the values shown in **Figure 3**. These initially calculated values (Figure 3A) are then converted to percentages (Figure 3B–D). PEGylated liposomes of 100 and 580 nm circulate well, with longer circulation times evident for the smaller 100 nm liposomes which, even after 3 days, had about 5% of the NPs still in circulation. The lack of a PEG layer or the presence of biotin decreases the circulation times of the liposomes, with the former being removed from the blood flow already 8 h after injection while the latter cease to circulate at about 48 h (Figure 3B,C). Further, NPs being expected to be long circulating, possessing a different surface chemistry such as polysarcosine and polyDMA ((poly(Sar-*b*-pCys(SO_2Et)) and poly(DMA-*b*-BzKetAc) NP), show relatively longer circulation times, especially the 41 nm NPs ((poly(Sar-*b*-pCys(SO_2Et)) and 65 nm poly(DMA-*b*-BzKetAc). After 3 days, these embryos still had 15% and 11.5% of the injected NPs still in circulation (3D).

3.2. Nanoparticle Circulation Time in Zebrafish and Mouse

So far, our analysis showed that NPs known from mice experiments to have short circulation times (non-PEGylated

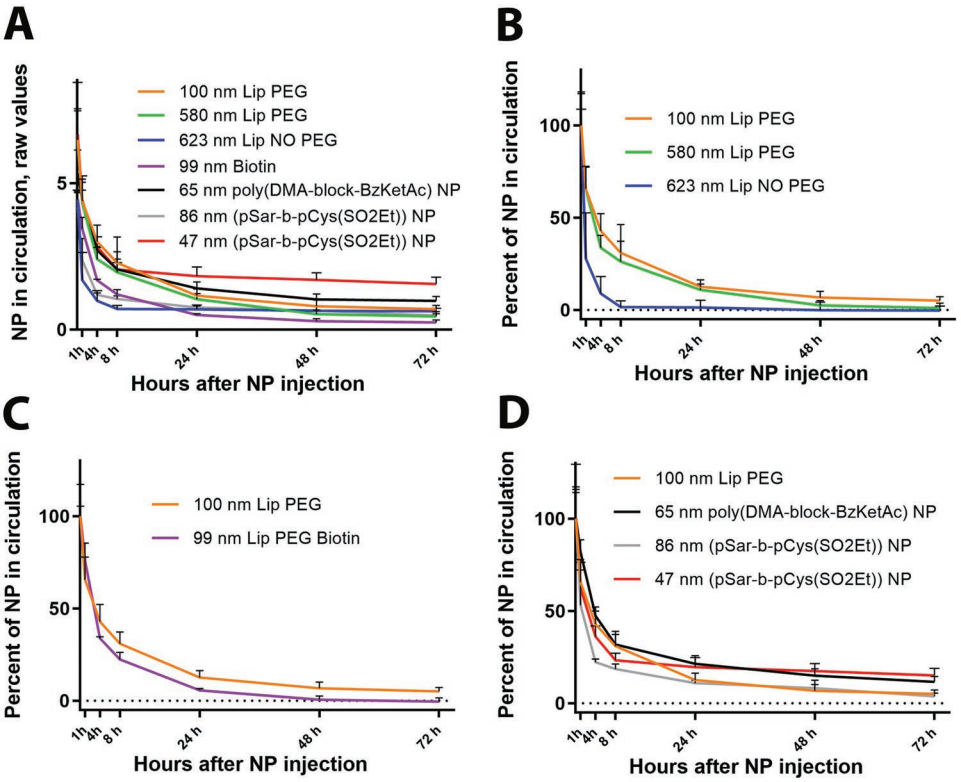

Figure 3. Quantification of the NP circulation times in zebrafish embryos. A) Raw values obtained by dividing the average fluorescence in the caudal artery with the total fluorescence. B–D) Values converted in percentages. B) PEGylated 100 nm liposomes are compared to 580 nm PEGylated liposomes and 623 non-PEGylated ones. C) The presence of biotin in PEGylated liposomes of about 100 nm is evaluated. D) NPs with three different surfaces known to allow long circulation (PEG, polyDMA, and polysarcosine) are compared. Bars indicate standard deviation, $N \geq 3$.

liposomes) or long circulation (PEGylated liposomes, polysarcosine NP, and polyDMA NP) behaved similarly in the zebrafish model. We therefore asked whether the zebrafish embryo could be used to predict NP circulation in mice; for this, we selected four of the analyzed NP mixtures (100 and 580 nm PEGylated liposomes, 623 nm non-PEGylated liposomes, and 47 nm (pSar-*b*-pCys(SO_2Et)) NP) and assessed their circulation in mice by estimating the residual fluorescence at four selected time points, 5 min, 4 h, 24 h, and 72 h. The comparison between these two sets of data is shown in **Figure 4**. In both animal models, non-PEGylated liposomes of about 623 nm were removed from the circulation in a matter of a few hours. PEGylated liposomes of 100 nm circulated better in both animal models than the 580 nm PEGylated liposomes, although in zebrafish both these liposomes circulated for longer times. The nanoparticles which performed best in both models were the 47 nm (pSar-*b*-pCys(SO_2Et)) NP with comparable circulation at 72 h. In the zebrafish, these NPs, after the first decline, remain stable in circulation, while in the mouse we observed a moderate decline throughout all the time points.

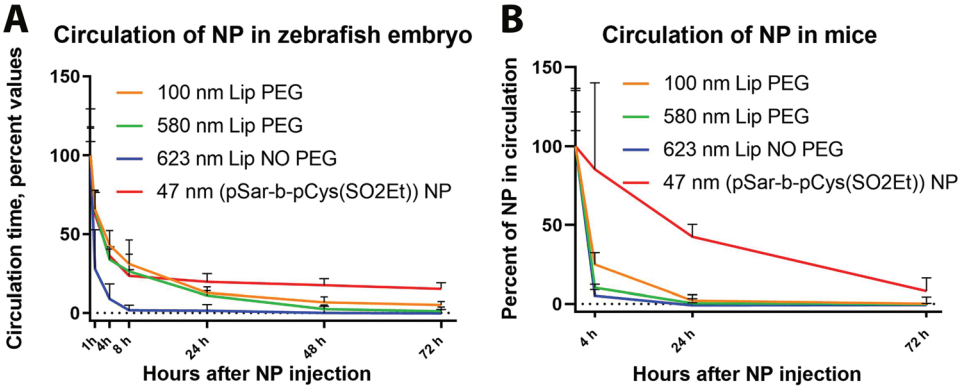

Figure 4. NP circulation in zebrafish embryos and mice. A) The circulation of the four selected NPs in zebrafish embryo: 100 and 580 nm PEGylated liposomes, 623 non-PEGylated liposomes, and 47 nm (pSar-*b*-pCys(SO_2Et)) NP. B) The circulation of the same NPs in the mouse model. $N \geq 4$.

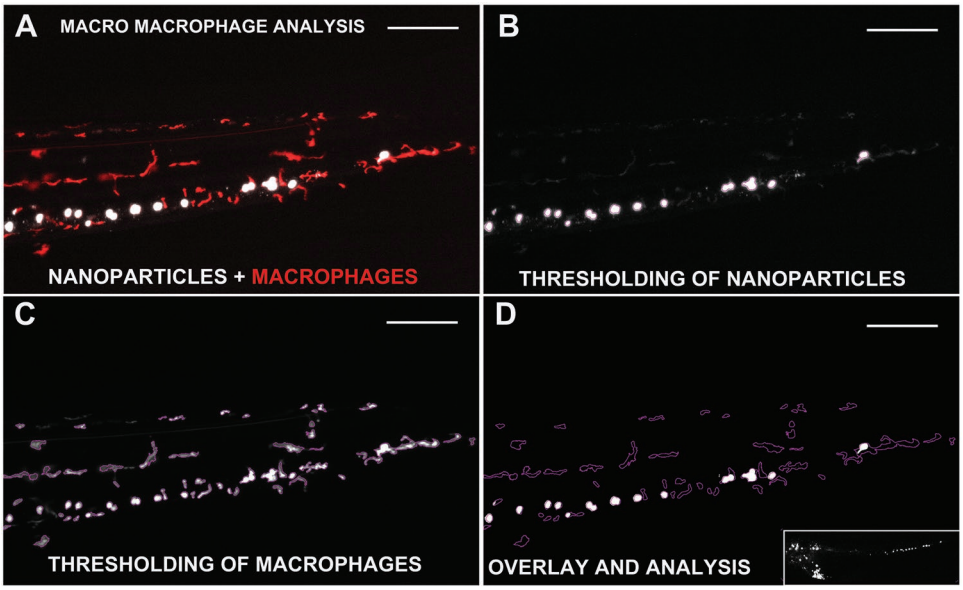

Figure 5. Macrophage uptake of NPs. Illustration of the steps undertaken by the MACRO for macrophage analysis to calculate the uptake of NPs. A) Zebrafish embryos injected with 623 nm liposomes without PEG (white) and fluorescent macrophages (red) are used for the analysis. B,C) NPs and macrophages are first thresholded, and D) their signals subsequently overlapped for analysis. The obtained values are normalized by the fluorescence of the whole zebrafish (panel (D), lower image).

3.3. Macrophage Uptake

The zebrafish embryo is an effective system to evaluate the uptake of NPs by macrophages (Figure 4A) which appear during development already by 24 h post fertilization;[25] for this evaluation it is essential to use a transgenic reporter line with fluorescent macrophages, here Tg(mpeg1:mcherry). The MACRO will first threshold the NP signal (**Figure 5**B), a necessary step in order to eliminate NPs that are still flowing from the evaluation, so that only the brightest NP accumulations are scored. The next step is the thresholding of the macrophages (Figure 5C), so that only the area occupied by these cells will be overlapped with that of the NPs (Figure 5D). Only the NPs found in macrophages are thereby scored for their fluorescence signals. As for all described analyses, this MACRO also evaluates the fluorescence signal of the whole fish and will save the measurements in two *.txt files.

Unlike for the circulation analysis, here the values are calculated as total rather than average fluorescence (RawIntDen rather than mean; see the "Experimental Section" for further details). For this, the macrophage uptake scoring is normalized relative to the overall zebrafish NP fluorescence. PEGylated liposomes of 100 and 580 nm, both poly(DMA-*b*-BzKetAc) NP and poly(Sar-*b*-pCys(SO_2Et)) NP, exhibit a very low uptake by macrophages (all with a score below 10), while non-PEGylated 623 nm liposomes and biotinylated liposomes 99 nm gave high values scoring over 20 and 30, respectively (**Figure 6**).

3.4. Endothelial Uptake of NPs

The use of the zebrafish line Tg(fli1a:EGFP) crossed with Tg(mpeg1:mcherry) allows for estimation of NPs uptake by endothelial cells (**Figure 7**A), a prominent characteristic of several NPs that we have tested in our zebrafish system. As for macrophage uptake, both NPs and macrophages have to be thresholded (Figure 7B,C), but in this case the signal derived from macrophage accumulations is removed (Figure 7D) and the remaining signal overlapped with that of the thresholded

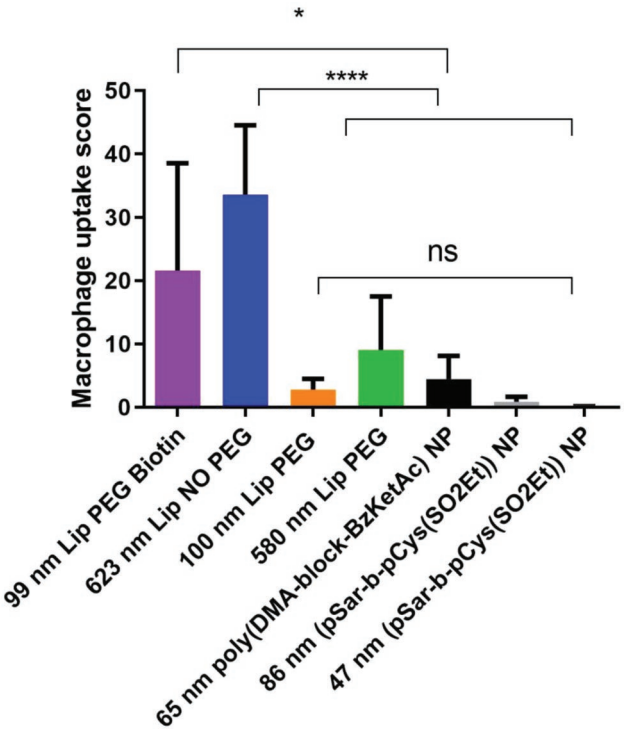

Figure 6. Quantification of NP uptake in the zebrafish by macrophages. The fluorescence scores of each NP are reported in arbitrary units. Statistics: one-way ANOVA with Tukey's multicomparison test: * = $P \leq 0.05$, **** = $P \leq 0.001$. Bars indicate standard deviation, $N \geq 6$.

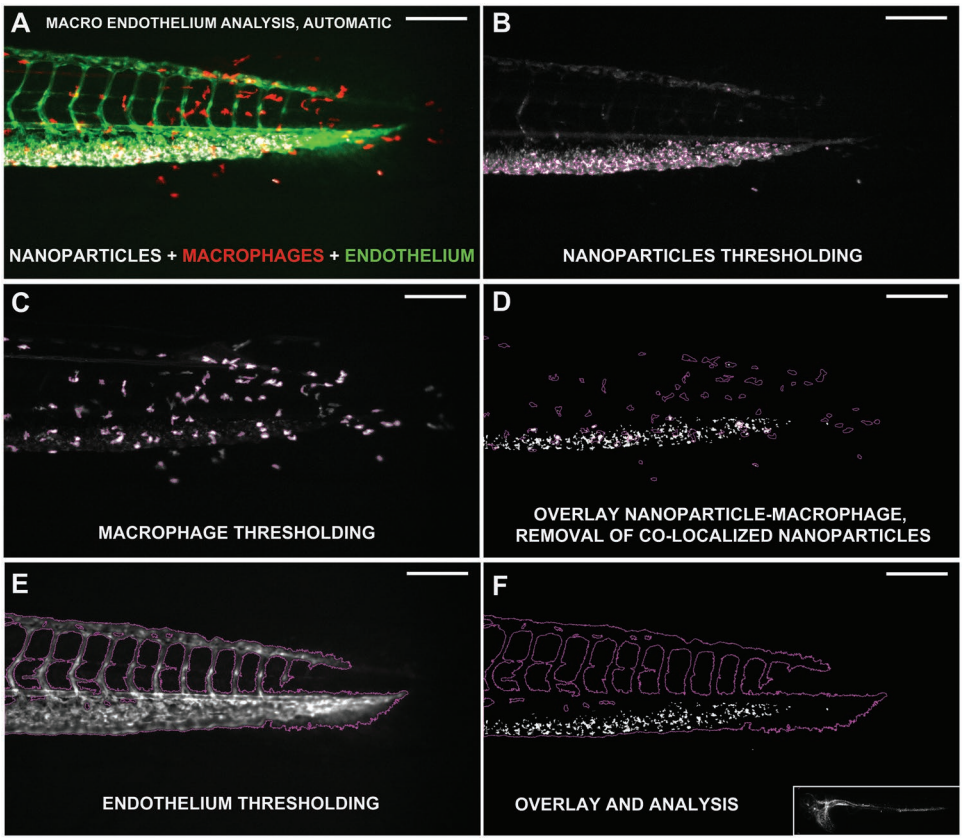

Figure 7. Endothelial uptake of NPs. Illustration of the steps undertaken by the endothelial analysis MACRO. A) Zebrafish embryos injected with 99 nm PEGylated liposomes with biotin (white) and fluorescent macrophages (red) as well as endothelium (green) are used for the analysis. B) NPs and C) macrophages are first thresholded. D) The NP signals in macrophages regions are deleted. Subsequently the signal of the endothelium is E) thresholded and F) overlapped to the residual NP measuring their fluorescence. The obtained values are normalized by the fluorescence of the whole zebrafish (panel (F), lower image).

endothelium in order to provide the final score (Figure 7E,F). As for macrophage uptake, the scored fluorescence intensity in the caudal vein has to be normalized relative to the whole fish total fluorescence signal; both these values are provided, for each zebrafish, in two *.txt files, one containing endothelial uptake score and the other the overall fluorescence signal.

Our results show that long circulating NPs such as PEGylated 100 nm liposomes, poly(DMA-*b*-BzKetAc) NPs, and both poly(Sar-*b*-pCys(SO_2Et)) NPs and for 623 nm non-PEGylated liposomes display a low value for endothelial cell uptake below 2. Biotinylated liposomes 99 and 580 nm liposomes instead exhibit large uptake values by endothelial cells which are significantly higher than the values of all other tested NPs (**Figure 8**) and above the value of 20.

4. Discussion

The vertebrate model zebrafish and the mouse model exhibit high genetic similarity with humans (70% of mouse and 82.2% of the zebrafish genes having a human orthologue)[26] while several important organs are also conserved in the fish, including the heart, brain, liver, kidney, pancreas, and intestine. Although the mouse remains the preclinical model of choice, in the field of nanomedicine, the zebrafish embryo possesses a number of advantages over the mouse model: 1) in the early development stages, the zebrafish is transparent, allowing precise imaging of the whole animal. 2) Several strains of this fish having fluorescent cell types are available so that their interactions with NPs can be easily studied. 3) The zebrafish maintenance costs are much lower than for mice with the estimate, from Boston University, of 1.05 $ for housing a single mouse while 0.25 $ for an entire tank (≈30 adults) of zebrafish.[27] 4) In addition, major differences are evident when it comes to the typical volumes of NPs that one needs to inject for experiments, allowing the researchers to save valuable material. Assuming the average weights of 1 mg for a zebrafish embryo and about 25 g for a mouse, 1 nL NP solution in zebrafish is equivalent to 25 µL in the mouse, a volume 25 000 higher. Despite these advantages, until now the use of the zebrafish has mostly been limited to the analysis of the toxic effects of NPs, especially on development.[28] An important limitation of the vast majority of these studies is that the NPs to be tested are administered only via the water bathing the fish which means the investigator has no control over the dose of NPs that access the vital organs. The only reliable method to overcome this is to microinject the NPs into the embryo, an operation which can be performed in different locations such as the yolk sac, the vasculature, intramuscular,

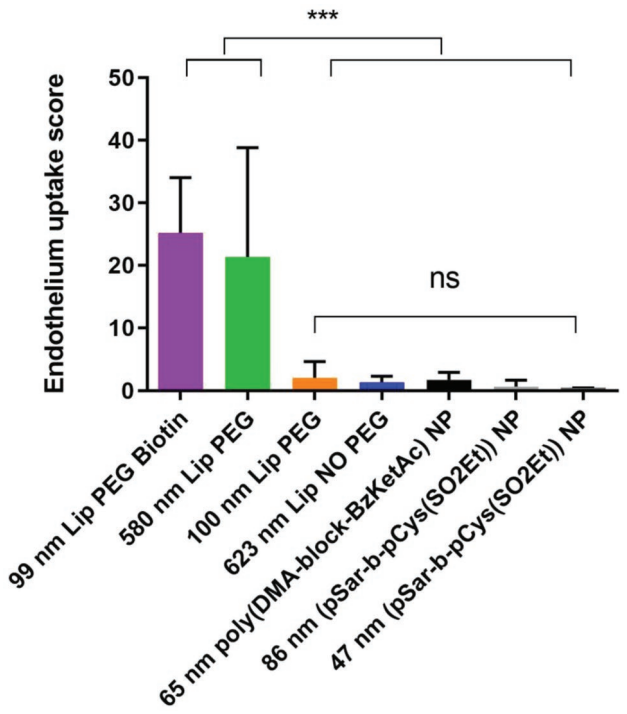

Figure 8. Quantification of NP uptake in the zebrafish by endothelial cells. The fluorescence scores of each NP are reported in arbitrary units. Statistics: one-way ANOVA with Tukey's multicomparison test: *** = $P \leq 0.005$. Bars indicate standard deviation, $N \geq 5$.

or into the hindbrain. In an earlier study, we have used vascular injection to analyze the toxicity of thioridazine, an antipsychotic drug whose promising therapeutic effects against *Mycobacterium tuberculosis* is hindered by its cardiotoxicity. We showed that although the free drug was highly toxic to fish embryos, the same drug concentration, encapsulated in poly(lactic-*co*-glycolic acid) (PLGA) NPs, resulted in no detectable toxicity, using multiple parameters.[29]

Over the past decade we have injected a significant number of different types of fluorescent NPs into zebrafish embryos and realized that for most NP types reproducible patterns of localization could be rapidly detected within a few hours after their injection. After intravenous injection, these patterns, at the extreme were, long or short circulation times and uptake or not by macrophages or vascular endothelial cells. Uptake by endothelial cells would be especially difficult to determine in mice. We were aware that if the zebrafish system is to become a standard model for screening NPs prior to their testing in preclinical mouse models, it would be essential to have available standardized methods for quantification of these different NP patterns. With this goal in mind, we introduce here a robust and simple methodology for reproducible quantification of these patterns for fluorescent NPs relative to their circulation times, and association with macrophages and endothelial cells. These parameters are of paramount importance when designing NPs for the treatment of different diseases. To our knowledge, the only method described in the literature to investigate NP circulation in zebrafish is the semiquantitative analysis proposed by Sieber et al.,[7] evaluating what they referred to as "circulation factor." That parameter is in fact not the actual NP circulation time but rather the ratio, limited to the caudal region, of NPs free flowing in the blood and the caudal vasculature area. In our method, however, we focused on the NP circulation by measuring the decrease of the average fluorescence in the caudal artery, a value which is then divided by the NP fluorescence in the whole zebrafish embryo. This last step of normalization, after transformation into percentages, allows us to obtain direct comparisons between different NPs and even when having different fluorescence intensity. Our method therefore provides an unbiased estimate of the NP circulation time.

With the method we introduced here, we analyzed NPs with a variety of sizes and materials. Our results clearly show that the behavior of NPs possessing a surface coating known to allow for long circulation times (in the range 1–3 days) in mammalian models, such as PEG, polysarcosine, polyDMA,[30–32] show the same behavior in the zebrafish. Importantly, a direct comparison of four selected NP formulations (100 and 580 nm PEGylated liposomes, 623 non-PEGylated liposomes, and 47 nm (pSar-*b*-pCys(SO_2Et)) NP) in the mouse and the zebrafish model revealed that the latter is able to predict with reasonable accuracy the pattern of circulation in mice. We believe that this animal model could be used in the future as an intermediate animal model, prior to the mouse, for testing different NPs having, for example, different surface chemistry. In the fish this could be done at a fraction of the cost in a shorter time.

We also quantified the uptake by macrophages in the zebrafish embryo and observed that NPs lacking surface coats such as PEG or polysarcosine and polyDMA, which are known to be rapidly removed from the circulation by macrophages[33] also exhibit the same behavior in zebrafish embryos; this was evident with our PLGA[4] or non-PEGylated liposomes in this study. Importantly, macrophage uptake, albeit greatly reduced for NPs containing PEG, polysarcosine and polyDMA, could still be observed in all tested NPs. The endothelial analysis also showed the importance of this cell type in determining the circulation of NPs. In particular, the presence of biotin in 100 nm PEGylated liposomes resulted in a high uptake by the endothelium, a behavior also observed in 580 nm PEGylated liposomes, a factor that could explain the reduced circulation times observed for these NPs when compared to plain 100 nm PEGylated liposomes. The mechanism that allows these NPs to be so efficiently taken up by the endothelial cells remains to be identified.

In this study, we did not address the uptake of NPs by neutrophils as; in our experience,[4,18] these cells play only a marginal role in the uptake of the NPs that we have tested after intravenous administration. However, in contrast to macrophages, neutrophils are known to be highly active in the uptake in surface-bound particles, such as bacteria following intramuscular injection of *Escherichia coli*.[34] Our MACRO could be easily customized to study this type of uptake since the zebrafish can be easily injected intramuscularly with NPs.

While our analysis was limited by uptake of NPs in macrophages and endothelial cells, the use of the method and MACRO that we have introduced here is by no mean restricted to these cells and could be easily adapted for analysis of any cell or tissue that can be labeled with a fluorescent protein. Of particular interest in the NP field would be the use of zebrafish

embryos with fluorescent liver,[35] kidney,[36] or heart.[37] Moreover, instead of injecting NPs, it would be possible to inject different types of bacteria and analyze their behavior in a vertebrate host based on quantification of their preferred cell or tissue niche. The generic method that we introduce here strengthens the importance of the zebrafish model as a screening tool for characterizing any type of fluorescent nanoparticles and thereby selecting a restricted number for the more time-consuming and expensive analysis in mammalian preclinical models.

5. Conclusion

The zebrafish embryo is rapidly becoming an important animal model for testing nanosized drug carriers and is capable of greatly reducing the number of formulations to be tested further in rodent animal models. Our study provides a robust instrument for unbiased and automated analysis of essential NP parameters during intravascular flow, thereby extending the advantages of the zebrafish embryo in NP research.

Acknowledgements

N.-J.K.D., A.K., and J.W. contributed equally to this work. The authors acknowledge the generous funding of the Kreftforeningen (Project No. 711091) and Norges Forskningsrådet (Project No. 275873 and Project No. 273319).

Conflict of Interest

The authors declare no conflict of interest.

Keywords

circulation time, macrophages, mice, nanoparticles, zebrafish

Received: December 2, 2019
Published online: January 15, 2020

[1] S. Sieber, P. Grossen, J. Bussmann, F. Campbell, A. Kros, D. Witzigmann, J. Huwyler, *Adv. Drug Delivery Rev.* **2019**, *151–152*, 152.
[2] S. Isogai, M. Horiguchi, B. M. Weinstein, *Dev. Biol.* **2001**, *230*, 278.
[3] L. Evensen, P. L. Johansen, G. Koster, K. Zhu, L. Herfindal, M. Speth, F. Fenaroli, J. Hildahl, S. Bagherifam, C. Tulotta, L. Prasmickaite, G. M. Maelandsmo, E. Snaar-Jagalska, G. Griffiths, *Nanoscale* **2016**, *8*, 862.
[4] F. Fenaroli, D. Westmoreland, J. Benjaminsen, T. Kolstad, F. M. Skjeldal, A. H. Meijer, M. van der Vaart, L. Ulanova, N. Roos, B. Nystrom, J. Hildahl, G. Griffiths, *ACS Nano* **2014**, *8*, 7014.
[5] P. L. Johansen, F. Fenaroli, L. Evensen, G. Griffiths, G. Koster, *Nat. Commun.* **2016**, *7*, 10974.
[6] F. Campbell, F. L. Bos, S. Sieber, G. Arias-Alpizar, B. E. Koch, J. Huwyler, A. Kros, J. Bussmann, *ACS Nano* **2018**, *12*, 2138.
[7] S. Sieber, P. Grossen, P. Detampel, S. Siegfried, D. Witzigmann, J. Huwyler, *J. Controlled Release* **2017**, *264*, 180.
[8] E. Blanco, H. Shen, M. Ferrari, *Nat. Biotechnol.* **2015**, *33*, 941.
[9] H. Chang, J. Y. Yhee, G. H. Jang, D. G. You, J. H. Ryu, Y. Choi, J. H. Na, J. H. Park, K. H. Lee, K. Choi, K. Kim, I. C. Kwon, *J. Controlled Release* **2016**, *244*, 205.
[10] F. Fenaroli, U. Repnik, Y. Xu, K. Johann, S. Van Herck, P. Dey, F. M. Skjeldal, D. M. Frei, S. Bagherifam, A. Kocere, R. Haag, B. G. De Geest, M. Barz, D. G. Russell, G. Griffiths, *ACS Nano* **2018**, *12*, 8646.
[11] J. M. Brown, L. Recht, S. Strober, *Clin. Cancer Res.* **2017**, *23*, 3241.
[12] A. R. Poh, M. Ernst, *Front. Oncol.* **2018**, *8*, 49.
[13] L. Pang, J. Qin, L. Han, W. Zhao, J. Liang, Z. Xie, P. Yang, J. Wang, *Oncotarget* **2016**, *7*, 37081.
[14] S. K. Patel, J. M. Janjic, *Theranostics* **2015**, *5*, 150.
[15] P. Zhao, W. Yin, A. Wu, Y. Tang, J. Wang, Z. Pan, T. Lin, M. Zhang, B. Chen, Y. Duan, Y. Huang, *Adv. Funct. Mater.* **2017**, *27*, 1700403.
[16] N. Abed, P. Couvreur, *Int. J. Antimicrob. Agents* **2014**, *43*, 485.
[17] G. Griffiths, B. Nystrom, S. B. Sable, G. K. Khuller, *Nat. Rev. Microbiol.* **2010**, *8*, 827.
[18] L. S. Ulanova, M. Pinheiro, C. Vibe, C. Nunes, D. Misaghian, S. Wilson, K. Zhu, F. Fenaroli, H. C. Winther-Larsen, S. Reis, G. Griffiths, *Dis. Aquat. Org.* **2017**, *125*, 19.
[19] L. Rizzello, J. D. Robertson, P. M. Elks, A. Poma, N. Daneshpour, T. K. Prajsnar, D. Evangelopoulos, J. O. Canseco, S. Yona, H. M. Marriott, D. H. Dockrell, S. J. Foster, B. De Geest, S. De Koker, T. McHugh, S. A. Renshaw, G. Battaglia, *bioRxiv* **2017**, https://doi.org/10.1101/119297.
[20] R. J. Mudakavi, S. Vanamali, D. Chakravortty, A. M. Raichur, *RSC Adv.* **2017**, *7*, 7022.
[21] R. Atanasiu, A. Radu, *Int. J. Pharm.* **1993**, *90*, 119.
[22] Z. Dong, J. Guo, X. Xing, X. Zhang, Y. Du, Q. Lu, *Biomed. Pharmacother.* **2017**, *89*, 297.
[23] J. R. McCarthy, P. Patel, I. Botnaru, P. Haghayeghi, R. Weissleder, F. A. Jaffer, *Bioconjugate Chem.* **2009**, *20*, 1251.
[24] K. Klinker, O. Schäfer, D. Huesmann, T. Bauer, L. Capelôa, L. Braun, N. Stergiou, M. Schinnerer, A. Dirisala, K. Miyata, K. Osada, H. Cabral, K. Kataoka, M. Barz, *Angew. Chem., Int. Ed.* **2017**, *56*, 9608.
[25] P. Herbomel, B. Thisse, C. Thisse, *Development* **1999**, *126*, 3735.
[26] K. Howe, M. D. Clark, C. F. Torroja, J. Torrance, C. Berthelot, M. Muffato, J. E. Collins, S. Humphray, K. McLaren, L. Matthews, S. McLaren, I. Sealy, M. Caccamo, C. Churcher, C. Scott, J. C. Barrett, R. Koch, G. J. Rauch, S. White, W. Chow, B. Kilian, L. T. Quintais, J. A. Guerra-Assuncao, Y. Zhou, Y. Gu, J. Yen, J. H. Vogel, T. Eyre, S. Redmond, R. Banerjee, J. Chi, B. Fu, E. Langley, S. F. Maguire, G. K. Laird, D. Lloyd, E. Kenyon, S. Donaldson, H. Sehra, J. Almeida-King, J. Loveland, S. Trevanion, M. Jones, M. Quail, D. Willey, A. Hunt, J. Burton, S. Sims, K. McLay, B. Plumb, J. Davis, C. Clee, K. Oliver, R. Clark, C. Riddle, D. Elliot, G. Threadgold, G. Harden, D. Ware, S. Begum, B. Mortimore, G. Kerry, P. Heath, B. Phillimore, A. Tracey, N. Corby, M. Dunn, C. Johnson, J. Wood, S. Clark, S. Pelan, G. Griffiths, M. Smith, R. Glithero, P. Howden, N. Barker, C. Lloyd, C. Stevens, J. Harley, K. Holt, G. Panagiotidis, J. Lovell, H. Beasley, C. Henderson, D. Gordon, K. Auger, D. Wright, J. Collins, C. Raisen, L. Dyer, K. Leung, L. Robertson, K. Ambridge, D. Leongamornlert, S. McGuire, R. Gilderthorp, C. Griffiths, D. Manthravadi, S. Nichol, G. Barker, S. Whitehead, M. Kay, J. Brown, C. Murnane, E. Gray, M. Humphries, N. Sycamore, D. Barker, D. Saunders, J. Wallis, A. Babbage, S. Hammond, M. Mashreghi-Mohammadi, L. Barr, S. Martin, P. Wray, A. Ellington, N. Matthews, M. Ellwood, R. Woodmansey, G. Clark, J. Cooper, A. Tromans, D. Grafham, C. Skuce, R. Pandian, R. Andrews, E. Harrison, A. Kimberley, J. Garnett, N. Fosker, R. Hall, P. Garner, D. Kelly, C. Bird, S. Palmer, I. Gehring, A. Berger, C. M. Dooley, Z. Ersan-Urun, C. Eser, H. Geiger, M. Geisler, L. Karotki, A. Kirn, J. Konantz, M. Konantz, M. Oberlander, S. Rudolph-Geiger,

M. Teucke, C. Lanz, G. Raddatz, K. Osoegawa, B. Zhu, A. Rapp, S. Widaa, C. Langford, F. Yang, S. C. Schuster, N. P. Carter, J. Harrow, Z. Ning, J. Herrero, S. M. Searle, A. Enright, R. Geisler, R. H. Plasterk, C. Lee, M. Westerfield, P. J. de Jong, L. I. Zon, J. H. Postlethwait, C. Nusslein-Volhard, T. J. Hubbard, H. Roest Crollius, J. Rogers, D. L. Stemple, *Nature* **2013**, *496*, 498.
[27] A. Weintraub, *Lab. Anim.* **2017**, *46*, 323.
[28] E. Haque, A. C. Ward, *Nanomaterials* **2018**, *8*, 561.
[29] C. B. Vibe, F. Fenaroli, D. Pires, S. R. Wilson, V. Bogoeva, R. Kalluru, M. Speth, E. Anes, G. Griffiths, J. Hildahl, *Nanotoxicology* **2016**, *10*, 680.
[30] V. D. Awasthi, D. Garcia, B. A. Goins, W. T. Phillips, *Int. J. Pharm.* **2003**, *253*, 121.
[31] T. Ishihara, T. Maeda, H. Sakamoto, N. Takasaki, M. Shigyo, T. Ishida, H. Kiwada, Y. Mizushima, T. Mizushima, *Biomacromolecules* **2010**, *11*, 2700.
[32] A. Makino, E. Hara, I. Hara, R. Yamahara, K. Kurihara, E. Ozeki, F. Yamamoto, S. Kimura, *J. Controlled Release* **2012**, *161*, 821.
[33] V. P. Torchilin, V. S. Trubetskoy, K. R. Whiteman, P. Caliceti, P. Ferruti, F. M. Veronese, *J. Pharm. Sci.* **1995**, *84*, 1049.
[34] E. Colucci-Guyon, J. Y. Tinevez, S. A. Renshaw, P. Herbomel, *J. Cell Sci.* **2011**, *124*, 3053.
[35] G. M. Her, Y.-H. Yeh, J.-L. Wu, *Dev. Dyn.* **2003**, *227*, 347.
[36] B. Perner, C. Englert, F. Bollig, *Dev. Biol.* **2007**, *309*, 87.
[37] E. de Pater, L. Clijsters, S. R. Marques, Y. F. Lin, Z. V. Garavito-Aguilar, D. Yelon, J. Bakkers, *Development* **2009**, *136*, 1633.